Mon. Not. R. Astron. Soc. **295,** 899–906 (1998)

Polarimetry of the eclipsing polar RX J0929.1 – 2404

David A. H. Buckley,[1] Lilia Ferrario,[2,3] Dayal T. Wickramasinghe[2,3] and Jeremy A. Bailey[4]

[1]*South African Astronomical Observatory, PO Box 9, Observatory 7935, Cape Town, South Africa*
[2]*The Astrophysical Theory Centre, School of Mathematical Sciences, The Australian National University, Canberra, ACT 0200, Australia*
[3]*Department of Mathematics, The Australian National University, Canberra, ACT 0200, Australia*
[4]*Anglo-Australian Observatory, PO Box 296, Epping, NSW 2121, Australia*

Accepted 1997 November 21. Received 1997 October 13; in original form 1996 July 3

ABSTRACT

We report polarimetric, spectropolarimetric and photometric observations of the eclipsing *ROSAT* cataclysmic variable RX J0929.1 – 2404, which confirm that the system is a new polar (AM Herculis system). This brings the number of eclipsing polars to nine, with RX J0929.1 – 2404 being only the third such system above the period gap. Circular polarization variations from ~ -20 to 10 per cent are seen over the 3.39-h orbital period, with a minimum around the time of eclipse. The photopolarimetric data were modelled using arc-shaped cyclotron emission regions in a centred dipole geometry. Results imply that RX J0929.1 – 2404 is a 'two-pole' system, with one emission region partially visible at all orbital phases. Spectropolarimetry observations show some evidence for the presence of cyclotron humps in the continuum, with spacings consistent with a magnetic field strength of $\sim$20 MG. Photometry of the eclipses provides information on the size of the emission region, which is consistent with a hotspot on the surface of the white dwarf. The eclipse duration implies an inclination in the range $70° \lesssim i \lesssim 78°$.

Key words: accretion, accretion discs – stars: individual: RX J0929.1 – 2404 – stars: magnetic fields – novae, cataclysmic variables – white dwarfs – X-rays: stars.

1 INTRODUCTION

The *ROSAT* soft X-ray and EUV surveys have been particularly successful in identifying new magnetic cataclysmic variables (CVs), and especially AM Herculis systems (polars), which now number $\sim$52, including several candidates yet to be confirmed as members of the class. The 29 or so new *ROSAT* discoveries (e.g. Wheatley et al. 1993; Beuermann & Schwope 1994; Beuermann & Burwitz 1995) have substantially altered our view of these objects as a group, and particularly the revised orbital period distribution. It is now unclear whether the orbital period 'gap' exists for the magnetic CVs (Buckley et al. 1993; Wu & Wickramasinghe 1993; Wu, Wickramasinghe & Li 1995), although this view is challenged (Kolb & de Kool 1993; Kolb 1995; Wheatley 1995). It is also apparent that the 'spike' at the lower edge ($P \sim 2$ h) of the gap is less statistically significant than it was in the pre-*ROSAT* era (Kolb & Ritter 1992; Wickramasinghe & Wu 1994). Indeed, Li, Wu & Wickramasinghe (1994a,b), Wu & Wickramasinghe (1993) and Li, Wickramasinghe & Wu (1995) have gone as far as suggesting that the angular momentum loss mechanism which drives the evolution is quite different for polars. They postulate a 'zero' or 'reduced' magnetic braking, where angular momentum losses are dominated by gravitational radiation. This contrasts with the disrupted magnetic braking mechanism, thought to operate in the majority of (non-magnetic) CVs (e.g. Mestel & Spruit 1987), where angular momentum loss is governed by magnetic braking with the secondary star's wind (at least for $P_{\rm orb} \gtrsim 3$ h).

A particularly important parameter in the evolution is the mass of the accreting white dwarf. In the conventional magnetic braking model, the white dwarf primaries in polars are required to have a rather restricted range in mass (e.g. Hameury, King & Lasota 1998a; Hameury et al. 1988b). Indeed, the period-gap systems could be explained only if they had particularly high masses (Hameury, King & Lasota 1991; Ritter & Kolb 1992), and in some instances their evolution could be quite different from most other polars, as in the case of QS Tel (RE 1938 – 461; Buckley et al. 1993).

It is well recognized that the most reliable method for

obtaining masses in binary systems is through the study of eclipsing systems. For the eclipsing polars, which following the discovery of RX J0929.1 − 2404 now number nine, not only is it possible in principle to derive such important parameters as the sizes and masses of the stellar components, but also the size, structure and location of the emitting regions associated with the accretion columns.

In this paper we present polarimetric and photometric observations of RX J0929.1 − 2404 (Sekiguchi, Nakada & Bassett 1994), suggested to be a polar. These data establish beyond doubt that it is indeed such a system. Furthermore, not only is it deeply eclipsing, but it is only the third eclipsing polar above the period gap, joining RX J0515.6 + 0105 ($P_{\rm orb} \sim 8$ h; Garnavich et al. 1994, Shafter et al. 1995, Walter, Wolk & Adams 1995) and EUVE J1429 − 38.0 ($P_{\rm orb} \sim 4.76$ h; Stobie et al. 1996). We show that the polarization and light curves are consistent with a 'two-pole' system with an accretion arc, associated with the dominant magnetic pole, which is observable over the whole orbital cycle. We present cyclotron emisson models consistent with the observed polarimetric and spectrophotometric data. The eclipse duration of ~ 8 min is ideally suited to detailed eclipse studies, although our limited eclipse data are insufficient to resolve more than one emission component. However, from ingress/egress times, we derive dimensions for the size of the emission region, and mass estimates for the white dwarf.

2 PHOTOPOLARIMETRIC OBSERVATIONS

White-light polarimetry of RX J0929.1 − 2404 was carried out on the SAAO 1.9-m telescope using the UCT Polarimeter (Cropper 1985) in 1994 February. The instrument consists of two rotating waveplates (1/4 and 1/2) and a Glan–Thomson prism analyser. Stepping motors control the rotation (at 10 Hz), and photon counts from a cooled RCA 31034A GaAs photomultiplier tube are accumulated in bins, with 100 bins per waveplate rotation. Fourier series are then fitted to the accumulated counts, and the four Stokes parameters (I, Q, U, V) derived from the 4θ, 6θ and 8θ terms. These are converted to polar co-ordinates (P, θ, V/I), and calibrated by observing polarized standard stars, and non-polarized stars through a set of linear and circular polaroids. Because of the photon-counting nature of the instrument, it is possible to perform high-speed photometry simultaneous with the Stokes mode (measuring *both* linear and circular) polarimetry, at a higher time resolution.

Our polarimetry observations of RX J0929.1 − 2404 were obtained with a 10-s resolution for the high-speed photometry and either 120- or 180-s resolution for the polarimetry. The star was observed on four nights in 1994 February, and the details of the dates, times, etc., appear in Table 1. All observations were obtained in essentially photometric conditions, although the seeing was poor (~ 2 arcsec) on two of the nights, which led to some light losses. Because of the faintness of the star ($V \gtrsim 17$), a small aperture was used: 6-arcsec diameter in poorer seeing and 4-arcsec diameter in good (< 1 arcsec) seeing. An automated off-set guider CCD camera was utilized to ensure accurate guiding.

On the last two nights, the polarimetry observations were interrupted a short time before an eclipse in order to perform higher speed photometry (0.5-s integrations) during the period of the eclipse. Two eclipses were observed with this method.

3 SPECTROPOLARIMETRIC OBSERVATIONS

In this section we present observations made with the AAO spectropolarimeter obtained on 1994 February 5. This instrument consists of the RGO Spectrograph used with a thinned Tektronix CCD detector and a modulator consisting of a rotating superchromatic quarter-wave plate. A calcite block analyser, positioned behind the slit, produces two spectra corresponding to orthogonal polarization states. Switching the quarter-wave plate between two positions which are 90° apart modulates these spectra according to the circular polarization. Each pair of exposures at the two plate positions was reduced to give intensity and V/I Stokes spectra using the Starlink TSP package (Bailey 1992).

We obtained a total exposure of 3000 s, with a spectral resolution of about 12 Å over the wavelength range 3600–7100 Å, before it clouded up. The resulting phase-averaged intensity and polarization spectra are shown in Fig. 1. The polarization spectrum shows positive circular polarization (up to a 2 per cent level), and the intensity spectrum shows some evidence for a slight modulation that could be attributed to the presence of cyclotron harmonics. We will see in Section 5 that this modulation can be explained by the presence of a magnetic field of about 20 MG, although this result should be taken with caution, since the data are not flux-calibrated and it is possible that these slow-scale variations could be caused by other factors.

4 REFINING THE ORBITAL PERIOD AND THE NATURE OF THE ECLIPSE

Fig. 2 shows four eclipses obtained on the nights of 1994 February 10, 13 and 14. The two lower curves are derived from the photopolarimetry runs (P9397 and P9398), and have a resolution of 10 s. The upper curves are from the 0.5-s high-speed photometric observations of the eclipse. The half-widths of the eclipses were used to determine the eclipse times, and these are given in Table 2, together with those measured from the CCD light curves of Sekiguchi et al. (1994). We have also included two more recent timings, kindly provided by Dr G. Schmidt.

A least-squares polynomial fit (order 1) to the times of minima gave the following eclipse ephemeris:

$$T_{\rm min\odot} = 244\,9007.5882 \pm 0.0002 + 0141\,243\,73 \pm 0.000\,000\,57{\rm E}. \quad (1)$$

Table 1. Observing log for RX J0929.1 − 2404.

DATE (day)	month	year)	RUN	HJD (- 2440000)	LENGTH (h)
9/10	Feb	94	P9393	9393.4404	4.40
10/11	Feb	94	P9394	9394.4730	3.84
13/14	Feb	94	P9397	9397.4167	4.76
14/15	Feb	94	P9398	9398.4888	2.90

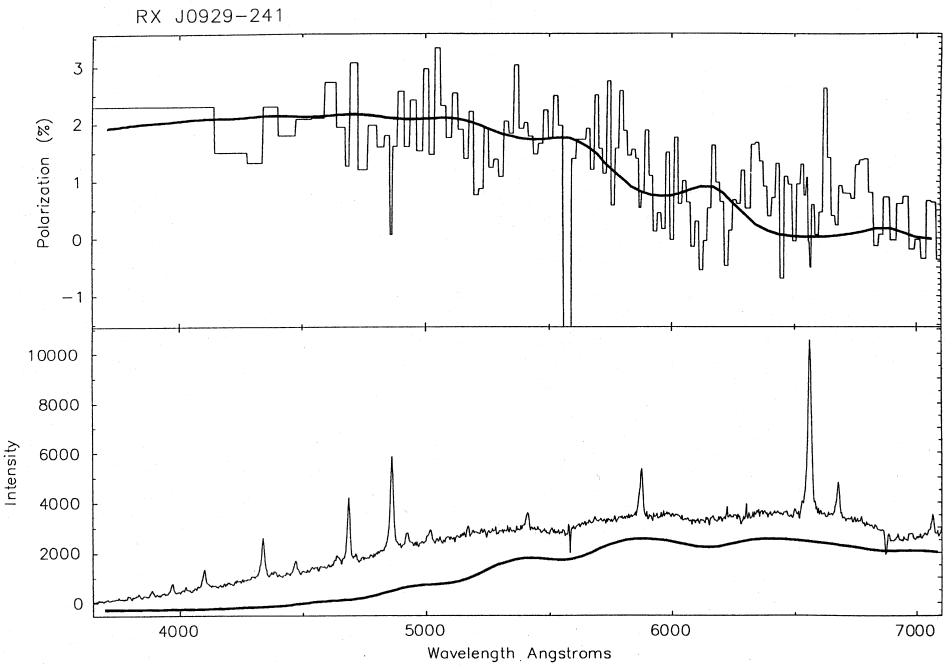

Figure 1. Phase-averaged AAT spectra for RX J0929.1 − 2404 obtained on 1994 February 5. Upper panel: polarization spectrum. Lower panel: intensity spectrum. The solid lines are our best-fitting models to the data. The viewing angle to the field direction is 85°, and the magnetic field strength is $B = 20$ MG.

The predicted times of minima, and the (O − C) residuals of this ephemeris, are included in Table 2 and displayed in Fig. 3.

Clearly, RX J0929.1 − 2404 is a totally eclipsing system, and the eclipses are reminiscent of such systems as UZ For (Bailey & Cropper 1991) and DP Leo (Bailey et al. 1993). The total phase (2nd to 3rd contact) lasts some ~ 450 s, or a phase width of 0.037. Clearly, the eclipsed source is entirely occulted during this interval. Unfortunately, the signal-to-noise ratio of the high-speed data is insufficient to allow us to resolve clearly the various possible contributors to the total luminosity of the system (e.g., the white dwarf, accretion spot and accretion stream). However, apart from the obvious sharp eclipse features, there are also indications of longer time-scale eclipse-related variations. For example, the two lower light curves of Fig. 2 both show more gradual declines preceding the sharp eclipse ingresses. Both light curves on JD 244 9397 and 244 9394 show evidence for a plateau-like phase on egress. We see from the higher signal-to-noise (but lower time resolution) photopolarimetric intensity data that the sharp eclipse ingress/egress can be as short as 10 s, although 20 s is probably a more typical estimate. The duration of egress may be more variable than ingress, judging from the (albeit lower quality) high-speed observations. We therefore conclude that there is some evidence for an eclipse of more than just one luminosity source, although the present quality of the data precludes a definitive derivation of the various dimensions of these components. High-time-resolution observations with superior signal-to-noise ratios are required to attempt a proper deconvolution of the eclipse into its various components.

Using 20 s as an upper limit of the sharp eclipse ingress/egress, we can estimate an average ingress/egress duration to be $\Delta\phi_{\rm ie} \lesssim 0.0016$, and the half-width of the eclipse (measured from mid-points of the ingress/egress curves) to be $\phi_{1/2} = 0.0192 \pm 0.0006$. This estimate comes from the four eclipses shown in Fig. 2, and the error estimate is the standard deviation, which is equivalent to 7.3 s of time. This uncertainty seems quite reasonable, given the individual errors which are typical ± 10 s. The stability of the eclipse ingress phase, and its brevity, argues in favour of the standard picture of an eclipse of a small, hot region on the white dwarf's surface. This hypothesis is preferred to the alternative eclipse-like 'dip' model, produced by absorption by the accretion stream (e.g. Watson et al. 1995). However, it is still possible that such absorption is present, and maybe associated with the slower ingress/egress components, or even the egress plateau.

5 MODELLING THE ECLIPSE

Although the quality of the eclipse data precludes definitive modelling, we will none the less use the above eclipse parameters to investigate implications regarding the system geometry and dimensions, as far as can be ascertained. We start with an estimate of the secondary star's mass, determined using the latest empirical mass–period and radius–period relationships as derived by Warner (1995), which imply $M_2/{\rm M}_\odot = 0.30$ and $R_2/{\rm R}_\odot = 0.35$.

The geometry of eclipses by Roche-lobe-filling secondary stars has been investigated by Chanan, Middleditch & Nelson (1976). The duration of total eclipse of the primary is a function only of the mass ratio, q, and inclination, i, but is not expressible in an analytical form. Horne (1985) presents a graphical form of the relationship, as a function of the eclipse width ($=2\phi_{1/2}$), and we use this to investigate the possible q–i 'phase-space' solutions for RX J0929.1 − 2404.

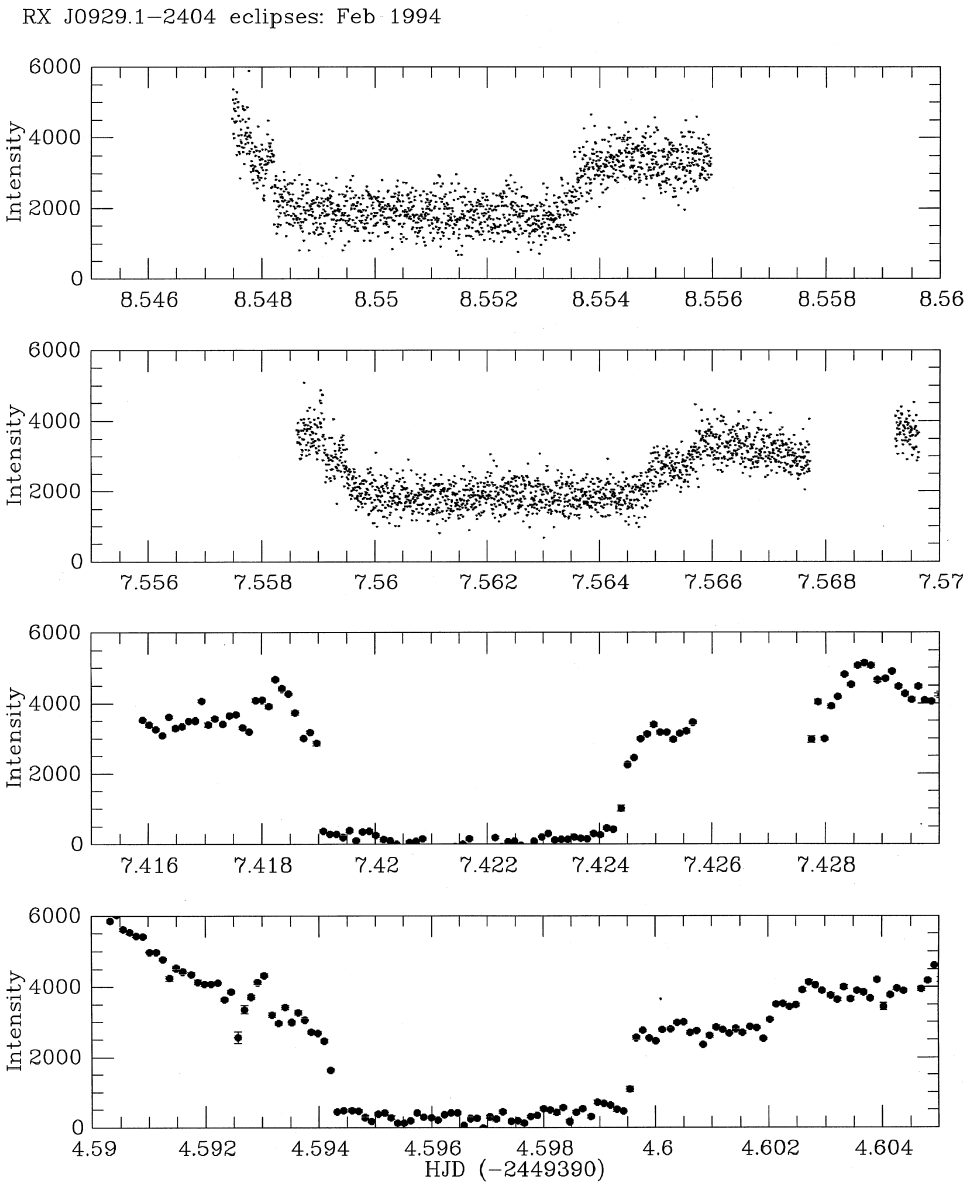

Figure 2. Four eclipse light curves of RX J0929.1 − 2404 from high-speed photometric ($\delta t = 0.5$ s; top curves) and photopolarimetric ($\delta t = 10$ s; bottom curves) observations on 1994 February 10, 13 and 14.

Table 2. Eclipse timings for RX J0929.1 − 2404.

CYCLE	OBSERVED	ERROR (days)	CALC.	(O − C) (days)
0	49007.589	0.001	49007.58826	0.00074
13	49009.424	0.001	49009.42442	-0.00042
14	49009.566	0.001	49009.56567	0.00033
21	49010.554	0.001	49010.55437	-0.00037
42	49013.521	0.001	49013.52049	0.00051
2760	49397.4210	0.0005	49397.42094	0.00006
2761	49397.5615	0.0002	49397.56218	-0.00068
2768	49398.5503	0.0002	49398.55088	-0.00058
7345	50045.02352	0.0010	50045.02342	0.00010
7804	50109.85462	0.0002	50109.85429	0.00033

Times in HJD − 240 0000.

Table 3. Parameters for RX J0929.1 − 2404.

q	i (°)	M_1 ($M_\odot$)	R_2/a	R_{L2}/a	a ($R_\odot$)	R_1	D ($10^9 cm$)
1.0	70.0	0.30	0.36	0.38	0.96	1.09	0.102
0.8	71.5	0.38	0.34	0.36	1.00	1.01	0.126
0.6	72.8	0.50	0.32	0.34	1.06	0.96	0.130
0.5	73.8	0.60	0.30	0.32	1.10	0.83	0.145
0.4	74.8	0.75	0.29	0.30	1.16	0.69	0.155
0.3	76.3	1.00	0.26	0.28	1.24	0.55	0.161
0.25	77.0	1.20	0.25	0.27	1.31	0.38	0.199
0.21	78.2	1.44	0.24	0.25	1.37		0.235

R_1 values from the mass–radius relation in Warner (1995) or, where appropriate, Buckley & Shafter (1995).

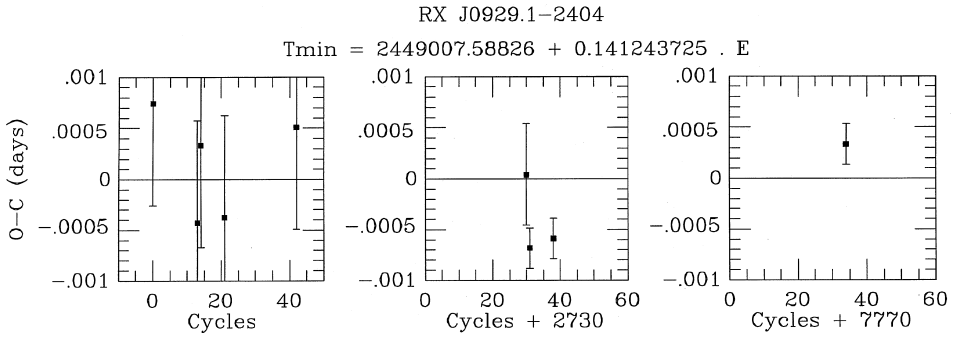

Figure 3. Residuals of the times of minima (Table 2) with respect to the best-fitting linear ephemeris.

For stable mass-loss from the secondary to the primary, we first require that $q(=M_2/M_1) \lesssim 1$. With $M_2 = 0.30\,\mathrm{M}_\odot$ and $\phi_{1/2} = 0.0192$, we find that the inclination must be in the range $70° \lesssim i \lesssim 78°$ for $0.30 < M_1 < 1.44\,\mathrm{M}_\odot$ (which is equivalent to $1.0 > q > 0.21$).

The eclipse duration also gives us a direct measurement of the size of the secondary, or rather its equivalent spherical radius. We use the well-known relationship (e.g. Buckley et al. 1990)

$$(R_2/a)^2 = \cos^2 i + \sin^2 i \, \sin^2 \phi_{1/2}. \quad (2)$$

This is derived with the assumption that the eclipsed source of light is in the orbital plane. In addition, we can use the formula for the volume radius of the secondary star Roche lobe (Eggleton 1983),

$$(R_{\mathrm{L}2}/a) = 0.49q^{2/3}/[0.6q^{2/3} + \ln(1 + q^{1/3})]. \quad (3)$$

Now we calculate the separation of the stellar components, from Kepler's law, which can be reformulated (in units of solar dimensions and days) as:

$$a_\odot = 4.2\,(M_1 + M_2)_\odot^{1/3}\,[P_{\mathrm{orb}}(\mathrm{d})]^{2/3}. \quad (4)$$

Using this with the estimates of the *relative* dimensions of the secondary (R_2/a) leads to absolute dimensions. In Table 3 we list the various parameters as a function of the mass ratio. We have included estimates of the white dwarf radius (R_1) from a mass–radius relation used by Buckley & Shafter (1995), which was derived from the Hamada–Salpeter relation for carbon white dwarfs in the mass range $0.5 < M_1 \lesssim 1\,\mathrm{M}_\odot$, namely

$$R_1/\mathrm{R}_\odot = 7.9 \times 10^{-3}\,(M_1/\mathrm{M}_\odot)^{-0.81}. \quad (5)$$

Included, for comparison and for the mass regime beyond the applicability of this equation, are estimates based on Warner's (1995) relationship, $R_1/\mathrm{R}_\odot = 0.0105\,(M_1/\mathrm{M}_\odot)^{-1/3}$.

Finally, we use the equation

$$D = \frac{\Delta\phi_{\mathrm{ie}}[M_1[1+q)]^{1/3} P_{\mathrm{orb}}^{2/3}\,(1-\alpha^2)^{1/2}}{0.0757} \quad (6)$$

given by Bailey (1990), generalized for an eclipse of *any* circular emission region (white dwarf photosphere, accretion spot, etc.). D is the radius of the *eclipsed* source, and α is a function of inclination given as $\alpha = \cos i/\cos i_{\mathrm{lim}}$, where i_{lim} is the minimum inclination allowable for a given value of q, i.e., for a grazing (non-total) eclipse. The units are in solar values for M_1 and D, and in days for P_{orb}, while Bailey (1990) provides a tabulation of i_{lim} as a function of q. The dimensions of the eclipsed source, based on the upper limit for $\phi_{\mathrm{ie}} = 0.0016$, is also shown in Table 3. We see that for all allowed values of the mass ratio $(0.21 < q < 1)$, the dimensions of the eclipsed light source contributing the most light to the system is always less than the actual size of the white dwarf. This is entirely consistent with the notion that a small 'hotspot' on the white dwarf, at the base of the accretion column, is the major contributor to the system luminosity, at least in the optical regime.

We note that for a given inclination, the radius of the secondary star as derived from the eclipse width (equation 2) is consistently lower than the equivalent Roche lobe volume radius (equation 3). The difference, which amounts to 5–8 per cent, can be readily explained if the projected distance of the hotspot from the centre of the secondary star is more than the projected distance of the white dwarf from the secondary. The assumption in equation (2), namely that the source of light is in the orbital plane, is no longer valid, and will lead to an underestimate in size of the secondary. It is equivalent to saying that the eclipse duration of the hotspot is less than for the white dwarf, because the limb of the secondary occults the source later, and uncovers it sooner than for the white dwarf. If we could clearly deconvolve the eclipse curves into the eclipse of the white dwarf and hotspot, we would be able to determine the exact line of latitude on the secondary where the eclipse takes place. As it is, it is clear that the discrepancy will become more acute at higher latitudes and for larger white dwarfs.

Can we now say anything about the likely range of white dwarf masses allowed in this model? If we can adequately restrict the inclination, then we can limit M_1. In the following section we argue that the best value for the inclination is $i = 75°$, and that larger values than this are unacceptable. This would limit M_1 to be $\lesssim 0.8\,\mathrm{M}_\odot$, although this may be model-dependent; we therefore avoid the temptation to use these polarization models to determine the white dwarf mass.

6 INTENSITY AND POLARIZATION BEHAVIOUR

The polarization and intensity data were binned on the orbital period according to the eclipse ephemeris (Section 4, equation 1), and the results are shown in Fig. 4. In this section we will attempt to interpret the position angle, intensity, linear and circular polarization data by assuming

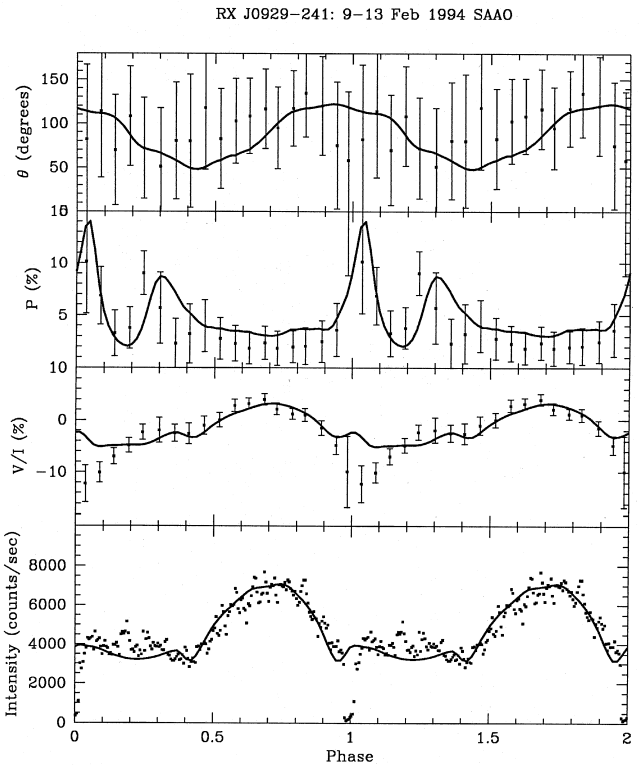

Figure 4. Phase-binned SAAO white-light polarization and intensity data for RX J0929.1 − 2404. From top to bottom: position angle of the linear polarization vector (θ); magnitude of linear polarization (P); circular polarization (V/I); intensity. The solid curves are the best models determined from the polarization data.

that the magnetic field structure of the white dwarf is that of a centred dipole, and then we will apply the models of Ferrario & Wickramasinghe (1990) to provide a fit to the data. Briefly, these models assume that the cyclotron emission regions consist of arcs that extend in magnetic latitude and longitude on the surface of the star. The total cyclotron emission is then derived by adding the emission from point sources which are distributed along the arcs and the contributions of which are weighted with their elementary surface area projected on to the plane of the sky. In these models, the optical depth parameter Λ is constant along each of these emission arcs, and the field strength varies according to

$$B=\frac{1}{2}\sqrt{(1+3\cos^2\theta)}, \tag{7}$$

where θ is the colatitude measured from the magnetic pole that is located in the hemisphere pointing towards the observer (see Ferrario & Wickramasinghe 1990 for a description of the parameters used in this section). The position and extension of the arcs is then modified until the theoretical curves match the observed intensity and polarization observations.

The data show that the sign of the circular polarization reverses for a significant fraction of the orbital phase, thus indicating that RX J0929.1 − 2404 is a 'two-pole' system with the observed radiation coming from two cyclotron emission regions located in two regions of opposite field polarity on the white dwarf surface.

The intensity curve shows that there is a dominant peak near phase 0.7 which is positively circularly polarized. We identify this region as the main cyclotron emission region. The data also show the presence of further local maxima between phases 0 and 0.4. In our model, these maxima arise from the secondary emission region.

The intensity peak near phase 0.7 occurs when the main cyclotron emission region comes into view from behind the body of the white dwarf. The peaks between phases 0 and 0.4 arise from the secondary emission region that is located in the observer's hemisphere and is never eclipsed by the body of the white dwarf. The latter region is also responsible for the negatively circularly polarized portion of the polarization curve, and for the occurrence of two linear polarization pulses detected near phases 0 and 0.25, when, respectively, the trailing and leading edges of this emission region are viewed near 90° to the magnetic field. In contrast, the emission region is viewed at small angles to the field between phases 0.5 and 1, resulting in weak cyclotron emission that becomes dominated by the radiation from the main pole that is visible at these phases.

In our modelling procedure, we attempt to determine the following quantities: the orbital inclination i, the colatitude of the magnetic axis θ_d, and the location and extent of the accretion arcs. We have assumed that the model has a polar field strength $B_p=20$ MG, consistent with what is found in most AM Hers. It should be noted that the magnetic field is not strongly constrained by the modelling of broad-band intensity and polarization data, particularly when only one waveband is considered. We have constructed a series of models by varying each of the above parameters while keeping the others fixed, and we have chosen a subset of models that give a reasonable and simultaneous fit to the observed position angle, linear and circular polarization, and intensity curves. The goodness of the fit was then estimated by eye. Our best-fitting model for this set of data is included in Fig. 4, where the theoretical curves are overlapped with the observations. The model has an orbital inclination $i=75°$ and a dipole tilt of $\theta_d=20°$. The effective harmonic number is $n=8$. Using the notation of Ferrario & Wickramasinghe (1990), the main emission region is below the orbital plane between $\theta_1=158°$ and $\theta_2=160°$, has a constant angular width $\Delta\theta=2°$, and is elongated towards the magnetic pole by 5°. The azimuthal extent is between $\psi_1=110°$ and $\psi_2=250°$. The electron temperature is $T_e=8$ keV, and the optical depth parameter is $\Lambda=10^6$, perpendicular to the stellar surface. The secondary emission region is located above the orbital plane between magnetic colatitudes $\theta_1=21°$ and $\theta_2=23°$, has a constant angular width $\Delta\theta=2°$, and is elongated towards the magnetic pole by 5°. The region extends in magnetic azimuth from $\psi_1=-150°$ to $\psi_2=150°$. The electron temperature of the shock is $T_e=8$ keV and $\Lambda=2\times10^5$.

The latitudinal and longitudinal uncertainties are typically of $\approx\pm10°$ in $\Delta\psi$ and $\approx\pm2°$ in $\Delta\theta$. We would like to remark that an inclination angle greater than that adopted by us has to be ruled out, since it would not give the correct positive-to-negative circular polarization ratio. This result is in good agreement with the inclination limits derived in the previous section from the eclipse width, with the maximum

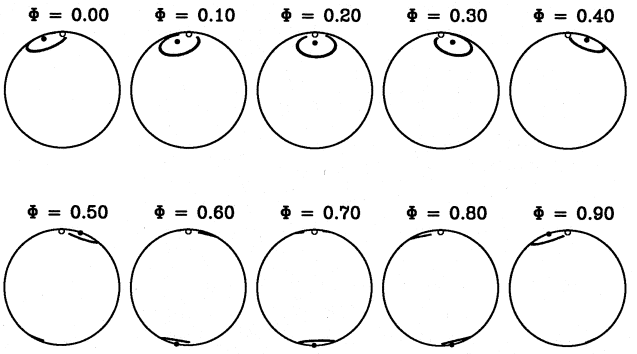

Figure 5. Position of the cyclotron emission regions as seen from Earth at 10 different phases. Open circle: spin axis; filled circle: dipole axis.

inclination allowed being 78° for a white dwarf mass less than the Chandrasekhar limit. In order to better visualize the results of our modelling, we have sketched in Fig. 5 the position of the cyclotron emission arcs as they are seen from Earth at 10 different orbital phases.

The theory of cyclotron emission predicts narrower and better defined cyclotron emission features as the viewing angle to the magnetic field approaches 90°. This means that cyclotron harmonics are more likely to be detected in those systems that are viewed, at least at some orbital phases, near 90° to the field direction. Given the high orbital inclination of RX J0929 − 241, both cyclotron emission regions may have portions of their arcs that are viewed, at some phases, near 90° to the field, so that cyclotron harmonics features are likely to be detected in the intensity spectrum. The spectropolarimetry observations presented in Section 3 appear to show a slight modulation of the continuum that could be attributed to cyclotron harmonics in emission. Although these features are very weak, we have nevertheless tried to fit a cyclotron spectrum to the data.

We have computed simple models following Wickramasinghe & Meggitt (1985), assuming a point source that is viewed at an angle of 85° to the field direction. The best-fitting spectrum has $B = 20$ MG, $T_e = 8$ keV and $\Lambda = 3 \times 10^7$. The resulting theoretical curves for the polarization and intensity spectra are included in Fig. 1. We note that since the spectrum is not flux-calibrated, the real stellar flux might not peak where it appears to in the uncalibrated data, but it might peak, for instance, further in the blue. If this were the case, higher values of the parameter Λ would be necessary to fit the overall spectral shape. Nevertheless, if the slow-scale variations in the intensity spectrum are of cyclotron origin, our magnetic field strength estimate would still hold, since the closeness of the cyclotron features allows us to put an upper limit of about 23 MG on the magnetic field strength.

7 THE ECLIPSING POLARS

RX J0929.1 − 2404 now joins two other eclipsing systems (RX J0515.6 + 0105 and EUVE J1429 − 380) above the 2–3 h period gap. In Table 4 we list the nine known eclipsing polars in order of orbital period, with determinations for various important parameters (inclination, masses, magnetic field strength), where available, as summarized by Bailey (1995).

8 CONCLUSIONS

Our polarimetric observations confirm RX J0929.1 − 2404 to be a new polar, with orbital period at 3.39 h, joining two other eclipsing systems above the period gap. The polarization variations have been successfully fitted using the arc-shaped cyclotron emission models of Ferrario & Wickramasinghe (1990). We find RX J0929.1 − 2404 to be a two-pole system with an orbital inclination $i = 75°$ and a dipole tilt $\theta_d = 20°$. The inclination is consistent with the observed eclipse parameters, which limits $i \lesssim 78°$ for realistic values of the white dwarf mass (i.e., $M_1 \lesssim 1.4\,M_\odot$), and adopting empirical period–secondary mass relations. While the spectropolarimetry is rather limited, and regrettably not

Table 4. Eclipsing polars.

Name	P_{orb} (days)	i (degrees)	M_1 ($M_\odot$)	M_2 ($M_\odot$)	B (MG)	References
RX J0515.6+0105	0.33292		$\lesssim 0.6$		62	[1]
EUVE J1429-38.0	0.19856	81	0.82	0.46_s		[2]
RX J0929.1-2404	0.14124	70-78	0.6-1.44:	0.30	20:	this study
UZ For	0.08787	86 ± 5	$0.7_p \pm 0.1, > 0.93_s$	0.14_p, 0.16_s	53, 75:	[3,4,5,6]
HU Aqr	0.08682	85 ± 5	$\sim 0.9_s$	$\sim 0.3_s$	37	[7]
WW Hor	0.08020	74 ± 5	0.7:			[8,9]
1H1752+081	0.07845	80 ± 2	$0.9 \pm 0.1_s$	0.185_s	7_z	[10,11]
EP Dra	0.07266	80:				[12]
DP Leo	0.06236	79.6	0.71_p	0.106_p	31, 59	[13,14,15]

s spectroscopic determination
z from Zeeman features
p photometric determination
[1] Shafter et al. (1995)
[2] Stobie et al. (1996)
[3] Ferrario et al, (1989)
[4] Bailey & Cropper (1991)
[5] Beuermann et al. (1988)
[6] Schwope et al. (1990)
[7] Schwope et al. (1993)
[8] Bailey et al. (1988)
[9] Beuermann et al. (1987)
[10] Barwig et al. (1994)
[11] Ferrario et al. (1995)
[12] Remillard et al. (1991)
[13] Biermann et al. (1985)
[14] Cropper & Wickramasinghe (1993)
[15] Bailey et al. (1993)

flux-calibrated, it is nevertheless consistent with the polarization modelling, and if the humps are interpreted as cyclotron features, then we derive a field strength of $\sim$20 MG.

Eclipsing systems are important in obtaining accurate parameters, and RX J0929.1 − 2404 will no doubt be useful in this respect, particularly given its long period. High-resolution photometry should be attempted with a larger aperture to enable a definitive deconvolution of the eclipse into its components. The data presented here indicate that the eclipse must be of a region considerably smaller than the white dwarf, and consistent with a hotspot at the base of the accretion column.

ACKNOWLEDGMENTS

We thank the AAT and SAAO staff for their technical support. Dr G. Schmidt kindly provided two recent eclipse timings. The referee provided useful comments, which have improved the paper.

REFERENCES

Bailey J., 1990, MNRAS, 242, 57
Bailey J., 1992, Starlink User Note 66
Bailey J., 1995, in Buckley D. A. H., Warner B., eds, ASP Conf. Ser. Vol. 85, Cape Workshop on Magnetic Cataclysmic Variables. Astron. Soc. Pac., San Francisco, p. 10
Bailey J., Cropper M., 1991, MNRAS, 253, 27
Bailey J., Wickramasinghe D. T., Hough J. H., Cropper M., 1988, 234, 19P
Bailey J., Wickramasinghe D. T., Ferrario L., Hough J. H., Cropper M., 1993, MNRAS, 261, L31
Barwig H., Ritter H., Barnbanter O., 1994, A&A, 288, 204
Beuermann K., Burwitz V., 1995, in Buckley D. A. H., Warner B., eds, ASP Conf. Ser. Vol. 85, Cape Workshop on Magnetic Cataclysmic Variables. Astron. Soc. Pac., San Francisco, p. 99
Beuermann K., Schwope A. D., 1994, in Shafter A. W., ed., ASP Conf. Ser. Vol. 56, Interacting Binary Stars. Astron. Soc. Pac., San Francisco, p. 119
Beuermann K., Thomas H.-C., Giommi P., Tagliaferri G., 1987, A&A, 175, L9
Beuermann K., Thomas H.-C., Schwope A. D., 1988, A&A, 195, L15
Biermann P. et al., ApJ, 293, 303
Buckley D. A. H., Shafter A. W., 1995, MNRAS, 275, L61
Buckley D. A. H., Sullivan D. S., Remillard R. A., Tuohy I. R., Clark M., 1990, ApJ, 355, 617
Buckley D. A. H., O'Donoghue D., Sekiguchi K., Chen A., Mason K. O., Kellett B. J., Hassall B. J. M., 1993, MNRAS, 262, 93
Chanan G. A., Middleditch J., Nelson J. E., 1976, ApJ, 208, 512
Cropper M., 1985, MNRAS, 212, 709
Cropper M., Wickramasinghe D. T., 1993, MNRAS, 260, 696
Eggleton P. P., 1983, ApJ, 268, 368
Ferrario L., Wickramasinghe D. T., 1990, ApJ, 357, 582
Ferrario L., Wickramasinghe D. T., Bailey J., Tuohy I. R., Hough J. H., 1989, ApJ, 337, 832
Ferrario L., Wickramasinghe D. T., Bailey J., Buckley D. A. H., 1995, MNRAS, 273, 17
Garnavich P. M., Szkody P., Robb R. M., Zurek D. R., Hoard D., 1994, ApJ, 435, L141
Hameury J.-M., King A. R., Lasota J.-P., 1988a, A&A, 195, L12
Hameury J.-M., King A. R., Lasota J.-P., Ritter H., 1988b, MNRAS, 231, 535
Hameury J.-M., King A. R., Lasota J.-P., 1991, A&A, 248, 525
Horne K., 1985, MNRAS, 213, 129
Kolb U., 1995, in Buckley D. A. H., Warner B., eds, ASP Conf. Ser. Vol. 85, Cape Workshop on Magnetic Cataclysmic Variables. Astron. Soc. Pac., San Francisco, p. 440
Kolb U., de Kool M., 1993, A&A, 279, L5
Kolb U., Ritter H., 1992, A&A, 254, 213
Li J., Wu K., Wickramasinghe D. T., 1994a, MNRAS, 268, 61
Li J., Wu K., Wickramasinghe D. T., 1994b, MNRAS, 270, 769
Li J., Wickramasinghe D. T., Wu K., 1995, MNRAS, 276, 255
Mestel L., Spruit H. C., 1987, MNRAS, 226, 57
Remillard R. A., Stroozas B. A., Tapia S., Silber A., 1991, ApJ, 379, 715
Ritter H., Kolb U., 1992, A&A, 259, 159
Schwope A. D., Beuermann K., Thomas H.-C., 1990, A&A, 230, 120
Schwope A. D., Thomas H.-C., Beuermann K., 1993, A&A, 271, L25
Sekiguchi K., Nakada Y., Bassett B., 1994, MNRAS, 266, L51
Shafter A. W., Reinsch K., Beuermann K., Misselt K. A., Buckley D. A. H., Burwitz V., Schwope A. D., 1995, ApJ, 499, 917
Stobie R. S., Okeke P. N., Buckley D. A. H., O'Donoghue D., 1996, MNRAS, 283, L127
Walter F. M., Wolk S. J., Adams N. R., 1995, ApJ, 440, 834
Warner B., 1995, Cataclysmic Variable Stars, Cambridge Astrophys. Ser. Vol. 28, Cambridge Univ. Press, Cambridge, p. 104
Watson M. G. et al., 1995, MNRAS, 273, 681
Wheatley P. J., 1995, MNRAS, 274, L51
Wheatley P. J., Watson M. G., Mason K. O., Buckley D. A. H., O'Donoghue D., 1993, in Regev O., Shaviv G., eds, 2nd Technion Haifa Conference, CVs and Related Physics. Institute of Physics, Bristol, p. 333
Wickramasinghe D. T., Meggitt S. M. A., 1985, MNRAS, 216, 857
Wickramasinghe D. T., Wu K., 1994, MNRAS, 266, L1
Wu K., Wickramasinghe D. T., 1993, Ann. Israel Phys. Soc., 10, 336
Wu K., Wickramasinghe D. T., Li J., 1995, Proc. Astron Soc. Austr., 12, 165